

ARMY RESEARCH LABORATORY



Fluorescence Spectra of Individual Flowing Airborne Biological Particles Measured in Real Time

Ronald G. Pinnick, Steven C. Hill, Stanley Niles, Yong-Le Pan, Stephen Holler, Richard K. Chang, Jerold R. Bottiger, Burt V. Bronk, Dominick C. Rozelle, Jay D. Eversole, and Mark Seaver

ARL-TR-1961

February 2001

Approved for public release; distribution unlimited.

The findings in this report are not to be construed as an official Department of the Army position unless so designated by other authorized documents.

Citation of manufacturer's or trade names does not constitute an official endorsement or approval of the use thereof.

Destroy this report when it is no longer needed. Do not return it to the originator.

Army Research Laboratory

Adelphi, MD 20783-1197

ARL-TR-1961

February 2001

Fluorescence Spectra of Individual Flowing Airborne Biological Particles Measured in Real Time

Ronald G. Pinnick, Steven C. Hill, Stanley Niles

Computational and Information Sciences Directorate, ARL

Yong-Le Pan

New Mexico State Univ.

Stephen Holler, Richard K. Chang

Yale Univ.

Jerold R. Bottiger

U.S. Army Edgewood Chemical Biological Center

Burt V. Bronk

U.S. Air Force Research Laboratory

Dominick C. Rozelle, Jay D. Eversole, and Mark Seaver

Naval Research Laboratory

Abstract

The UV-excited fluorescence spectra of individual flowing biological aerosol particles as small as 2 μm in diameter have been measured in real time (rates up to 10 particles per second). The particles are illuminated with a single shot from a Q-switched 266- or 351-nm laser. The signal-to-noise ratio and resolution of the spectra are sufficient for observing small line-shape differences among various types of bioaerosols (e.g., bacteria versus pollens) and between the same types of bioaerosol prepared under different conditions (e.g., the unstarved and four-month-starved *E. coli* strain DH5). Multiple-wavelength excitation provides additional information for distinguishing bioaerosols based on their fluorescence spectra.

Army Research Laboratory

Adelphi, MD 20783-1197

ARL-TR-1961

February 2001

Approved for public release; distribution unlimited.

Contents

1. Introduction	1
2. Experimental Setup	3
2.1 Biological Samples	5
2.2 Aerosol Generation	6
3. Results and Discussion	7
3.1 Spectra From Uniform Particles	7
3.2 Spectra From Bacterial Particle Aggregates of Different Sizes	8
3.3 Spectra of Similar Bacteria Prepared Under Different Conditions	9
3.4 Spectra of Pollens and Bacteria	11
3.5 Spectra for Multiwavelength Excitation	12
3.6 Advantages and Limitations of This Technique	13
4. Conclusion	15
Acknowledgments	16
References	17
Distribution	21
Report Documentation Page	25

Figures

1. Schematic of the experimental setup used for detecting single-shot laser-induced-fluorescence spectra from individual micrometer-sized aerosol particles	4
2. Frequency-of-occurrence histogram distributions of peak intensity for 1000 consecutive fluorescence spectra of individual tryptophan particles	7

3. Single-particle laser-excited fluorescence spectra from clusters of airborne <i>B. subtilis</i> vegetative cells with nominal diameter 5 μm , 2.3 μm , and 1.8 μm	9
4. Single-particle, 266-nm laser excited fluorescence spectra from nominal 5- μm -diam clusters of <i>B. subtilis</i> var. <i>niger</i> spores, and <i>B. subtilis</i> var. <i>niger</i> vegetative cells	10
5. Fluorescence spectra of starved and unstarved <i>E. coli</i> strain DH5 ...	10
6. Single-shot, single-particle fluorescence spectra from nominal 5- μm -diam clusters of paper mulberry pollen, meadow oat pollen allergen, and <i>E. coli</i> , and their corresponding 100-particle accumulation spectra	11
7. Fluorescence spectra of <i>B. subtilis</i> var. <i>niger</i> vegetative cells and <i>A. versicolor</i> fungal spores	12

1. Introduction

Bioaerosols [1–5] have been studied in and around workplaces, homes [5], hospitals [6,7], buildings with defective air-handling systems, factories where metal-working fluids are used [8], pig farms [9], dairies [10] and other animal houses [4], agricultural operations, sites of sludge application [11], recycling and composting plants [12], and sewage treatment plants. Unlike most common atmospheric aerosols, some airborne microorganisms can cause infectious diseases. Like other biological aerosols (e.g., dust mite allergens) and nonbiological aerosols (e.g., diesel exhaust particles [13]), they can also cause allergies and other respiratory problems.

Improved methods for measuring biological and other aerosols are needed. In this report “real time” indicates the capability of sampling a particle within 0.1 s. Presently, methods that measure aerosol size distributions in real time provide almost no information about particle types* and cannot specifically identify particular microorganisms. On the other hand, methods that specifically identify microorganisms and/or proteins in a sample are generally time-consuming and require aerosols to be collected [14–19]. Furthermore, for most allergens, toxins, and microorganisms, specific identification requires culturing the sample or using specific protein or nucleic acid recognition molecules.†

Instruments that run continuously and classify particles into broad classes of biological and other aerosols (and also determine size distributions of the particles in each class) would have several advantages:

- (1) In monitoring harmful bioaerosols, a rapid response may be necessary in situations where it would be impractical to continuously run an identifier (impractical because of requirements for reagents and for the collection of particles). For example, a continuously running monitor/classifier could indicate when to sample for and identify specific harmful bioaerosols. Also, in searching for or studying of intermittent sources of bioaerosols, a rapid response is necessary.
- (2) Recognition molecules are not always available for all particle types of interest.
- (3) Improved studies of bioaerosol dynamics and reactions (agglomeration, nucleation [20], evaporation, growth, mixing, etc) may require a real-time monitoring capability.

*Single particle mass spectrometry and the intrinsic fluorescence-based methods discussed here are exceptions. Single-particle x-ray dispersive analysis methods require sample collection.

†Some pollens or other particles that can be identified microscopically are exceptions.

Fluorescence particle counters that continuously measure the laser-induced intrinsic fluorescence (total or spectrally dispersed) from individual bioaerosol particles have been shown to be able to partially discriminate between biological and nonbiological aerosols [21–27]. Because the biological particles of interest may occur as very minor or rare species entrained within a main population of nonbiological particles, the fluorescence must be measured for each particle so that signals are uncontaminated and undiluted by those of the main population.

Classification with the use of only intrinsic fluorescence spectra is challenging:

- (1) There are so many possible types of biological aerosol particles.
- (2) Naturally occurring biological aerosols may be mixtures of several types of particles and compounds.
- (3) Differences between the emission spectra of highly purified bacterial or protein samples may be small (spectra may be dominated by a small number of primary fluorophors).
- (4) Differences in spectra may depend upon growth conditions, the atmospheric environment (e.g., temperature, humidity, and sunlight), and other factors.

We report a method for measuring high-quality, reproducible, single-shot, ultraviolet- (UV)-excited fluorescence spectra of individual airborne biological particles. Particles are interrogated by a pulsed UV laser [22,23] as they are carried by a stream of air through a small sample region defined by the intersection of two focused continuous-wave (cw) diode-laser beams [27]. This report extends the findings reported in our recent letter [27] and shows that (a) single-shot spectra of particles (which are aggregates of bacteria) as small as 1.8 μm in diameter can be measured, (b) particles within certain size ranges can be selected for measurement, (c) differences between spectra of bacteria of a single species grown under different conditions can be seen in single-particle spectra, and (d) biological aerosols that have almost identical single-shot fluorescence spectra when excited at 266 nm can have 351-nm-excited spectra that differ significantly from each other. Our results suggest that single-shot spectra from individual bioaerosols can be measured and may be useful for continuous detection and partial characterization of biological aerosols.

2. Experimental Setup

Our goal is to demonstrate a method for the real-time measurement of single-particle fluorescence spectra for characterization of biological particles. However, we need to be able to measure single-particle fluorescence spectra with good signal to noise before we can prove the utility of spectra. This is technically challenging for several reasons. First, fluorescence signals are very weak: we are trying to detect fluorescence from single particles containing only a few picograms of material, and only a small fraction of the mass of biological particles consists of fluorophors. Second, because particles are mixed randomly in the air, particles moving rapidly through an optical sample volume occur at random times, and so we must be able to measure spectra of particles as they appear at random times; further, particles of interest may exist as a small concentration in a far higher concentration of nonbiological aerosols. Third, the fluorescence spectra from various biological and nonbiological particles extend over a wide wavelength range, from the UV to the visible and near-infrared (IR) regions (280 to 750 nm). We want to excite particles in the UV wavelength and where most biological particles (and biological molecules) have a high absorption and fluoresce efficiently.

Our strategy to overcome these technical difficulties [22,23,25,27] has several key elements: First, we use a focused pulsed UV probe laser, which is triggerable on demand and has a sufficiently high intensity to excite measurable fluorescence in microparticles. Second, to increase our fluorescence collection ability, we use a large numerical aperture (NA) reflecting objective that can collect fluorescence from the emitting particle over a large solid angle and focus it onto the slit of a spectrograph without chromatic aberration. Third, to sense the fluorescence at the exit port of the spectrograph, we use an intensified charge-coupled device (CCD) detector (ICCD), which is gated on only during the laser pulse so that it records the fluorescence of the targeted particles alone, undiluted and largely uncontaminated by background. Finally, the focused probe laser and large NA collection objective demand a tiny sample volume. To define a small sample volume through which particles must traverse to be sampled, we require that particles pass through crossed cw diode-laser beams that are focused immediately upstream from the UV probe laser.

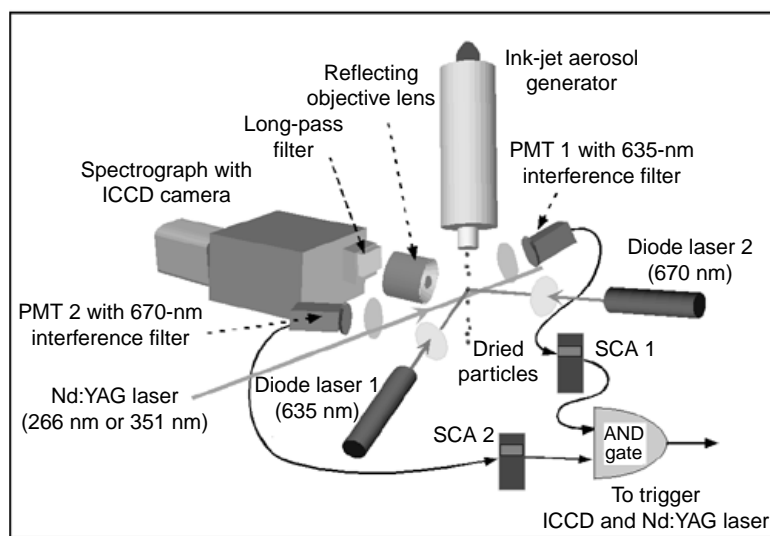
The key equipment is as follows. The Q-switched UV laser output is either the 266-nm fourth harmonic of an Nd:YAG laser, 30- or 70-ns pulse duration (Spectra Physics, model X-30 or Y-70 with the 532-nm output converted to 266 nm by a beta-barium borate doubling crystal from Superoptronics), or the 351-nm third harmonic of an Nd:YLF laser, 120-ns pulse duration (Quantronix). The Q-switched laser fires within $\sim 3 \mu\text{s}$ of the trigger pulse. The Schwarzschild reflecting objective (Ealing) has a 0.5 NA. The

spectrograph (Acton model SP-150, NA = 0.125) has a 300-groove/mm grating blazed at 500 nm. The input slit width is 1 mm (resolution is about 4 nm). The ICCD camera (Princeton Instruments, ITE/CCD-1024MLDS-E with PG200 pulse generator) is a fiber-optic-coupled, thermoelectrically cooled ICCD gateable to 50 ns with 1024 × 256 pixels. The ICCD's image intensifier acts as a fast shutter, opening when the targeted particle is illuminated by the UV laser. A long-pass filter is placed in front of the spectrograph to block elastically scattered light of the UV laser and to pass the fluorescence. A liquid cell containing N, N-dimethyl formamide is used to absorb the 266-nm light.

Figure 1 illustrates schematically our experimental setup. Particles entrained within a stream of air are directed downward toward the sample volume. In the experiments reported here, there is no air-tight chamber, and so the air stream is blown into the system toward the sample volume.

The requirement for a precisely defined sample volume is met by the use of two nearly orthogonal, different-wavelength diode-laser beams (diode lasers (LaserMax) 1 and 2 emit at 635 and 670 nm). These lasers define a 15- μm -diam volume centered in the focal plane of the reflecting objective (the beams are crossed so that the focal volume is approximately spherical). As an aerosol particle flows through the focal volume of the crossed beams, the near-forward elastic scattering is measured with photomultipliers PMT 1 and PMT 2 (with narrow-band interference filters at 635 and 670 nm). The PMT signals are fed into two single-channel analyzers (SCA 1 and SCA 2)

Figure 1. Schematic of the experimental setup used for detecting single-shot laser-induced-fluorescence spectra from individual micrometer-sized aerosol particles. Sample volume is defined by two intersecting cw diode-laser beams (at 635 and 670 nm). When a particle traverses the sample volume, (1) it scatters the light from



two diode laser beams; (2) this light is detected by photomultipliers PMT 1 and PMT 2; (3) if signals from each PMT fall within preset voltage windows, each single-channel analyzer produces an output; (4) if outputs of both SCAs are logical ones, the AND gate indicates that a spectrum is to be measured for this particle (by sending a triggering signal to the UV laser and ICCD); (5) Q-switched UV laser fires and excites fluorescence in the particle; (6) the fluorescence is collected by the reflecting objective and focused onto the input slit of spectrograph; (7) the spectrograph disperses energy; and (8) the spectrum is recorded with ICCD, which is gated to be on when the UV laser fires.

set to operate as discriminators in a window mode. We ensure that the particles have sizes within a certain range by requiring the intensity of the diode-laser light scattered by the particle (assumed to increase with particle size) to fall within a preset interval. The two SCA outputs are fed into a logical AND gate, which produces an output pulse only when the two SCAs' output signals overlap for at least 3 ns. The AND gate output then sends a trigger pulse to the Q-switched laser and the controller of the ICCD; i.e., particles must pass through the intersection of both focused-trigger beams before a logic pulse triggers the UV laser to fire and the ICCD to turn on. Thus, the system ignores particles not flowing through this intersecting region (which may not be illuminated by the central portion of the UV laser beam and may not be in the focal region of the reflecting objective).

2.1 Biological Samples

Several of the samples were used as purchased: meadow oat pollen allergens (Greer Laboratory), paper mulberry pollen (Duke Scientific), *Bacillus subtilis* (lyophilized cell that are probably cells, American Type Culture Collection (ATCC) 6633, Sigma Chem.), *B. subtilis* var. *niger* spores (Dugway Proving Ground, UT), *Erwinia herbicola* (ATCC 33243), and fungal spores (*Aspergillus versicolor*, ATCC 9577).

B. subtilis var. *niger* (lyophilized cells) and *E. herbicola* were grown by streaking onto tryptic soy agar plates. *E. coli* strain DH5 was maintained on glucose M9 minimal media agar (Sigma Chemical Co., St. Louis, MO) enriched with thiamine (Fisher Scientific, Pittsburgh, PA) [28]. For sample preparation, 1-ml aliquots from overnight cultures were transferred to sterile 1.5-ml polypropylene microcentrifuge tubes. Cells were gently pelleted, the supernatant fluids were removed, and the pellets were gently suspended in 1 ml of sterile 0.9% NaCl. The washing process was performed three times to ensure removal of all nutrient media [29]. Viable but not culturable bacteria were grown and measured as described in Roselle et al [30] (see next paragraph), except that 50-ml cultures of bacteria in minimal media were grown to a stationary phase and then stored in the dark at room temperature in the original flasks without further manipulation for four months.

To characterize the aged cells, we began by centrifuging 1-ml aliquots for 5 min at 4000 rpm to remove larger (viable and culturable) bacteria. The supernatant fluid was isolated, the pellet was resuspended in 0.9% NaCl, and the supernatant fluid was centrifuged for 15 min at 14,000 rpm to pellet the smaller bacteria. Again the supernatant fluid, which contained small unpelleted bacteria (<0.5 μm), was isolated, and the remaining pellet was resuspended in 0.9% NaCl. A portion of this last supernatant fluid was further processed by a Centricon 100 concentrator that elutes soluble components (less than 100,000 MW) through a membrane into a lower collection chamber while retaining the small bacteria in the upper chamber. The separation procedures just described yield four samples (a pellet of larger bacteria, a pellet of smaller bacteria, a supernatant fluid with smallest bacteria,

and the effluent from the Centricon concentrator). The number of colony-forming units from each *E. coli* sample was determined by serial dilution titers and plating onto LB agar. Direct counts were done with acridine orange stain and epifluorescence microscopy as described elsewhere [30,31]. Direct viable counts were also done, as previously described, by incubation of bacterial samples in 0.25 g/l YT media and 20 g/ml naladixic acid (which inhibits cell division but not cell growth) for 24 hr, followed by acridine orange staining [30,32]. The samples were visually examined for growth by epifluorescence microscopy, and elongated cells were counted.

2.2 Aerosol Generation

An ink-jet aerosol generator (IJAG) [33] was used to generate test aerosols. It produces dry aerosol particles that are somewhat monodispersed (the typical standard deviation in size distribution is 15 percent). The material to be aerosolized in the IJAG is suspended in distilled, deionized, and filtered water and then inserted into an ink-jet cartridge (HP 51612A, purchased empty) having 12 nozzles. Each cartridge nozzle can be activated through its resistive heater to generate a droplet approximately 50 μm in diameter, plus one or two smaller satellite droplets. Droplets are generated sequentially in the 12 nozzles at a frequency selected to be between 1 Hz and 2 kHz, or singly on demand. These droplets are fired downward, carried by a filtered stream of air, and passed through a drying chamber heated to about 104 °C. As these droplets traverse the drying chamber, their water component evaporates, leaving the residual particles, which dry into roughly spherical aggregates. Smaller aggregates produced from the satellite droplets are swept out of the drying chamber by a purge flow system. Because the size of the primary ink-jet droplet is fixed, the size of the dried particle depends only on the initial sample concentration in the water suspension. For this series of measurements, we have in most cases prepared 0.1-percent suspensions by weight, resulting in 5- μm -diam dried particles. A dedicated controller operates the ink-jet cartridge and drying chamber. At the exit port of the generator, the dried particles are carried in an air stream through a tapered 1-mm-diam exit nozzle.

An aerodynamic particle sizer (TSI, Inc., model 3310A) was used to provide an aerodynamic size distribution of the particles in real time. In most cases, the sizes were also measured through scanning electronic microscope (SEM) images of particles collected on filters.

3. Results and Discussion

3.1 Spectra From Uniform Particles

We initially tested the apparatus with tryptophan aerosols. Tryptophan is highly absorbing at wavelengths below 295 nm, has a relatively large fluorescence quantum efficiency (0.1 to 0.2), and makes up 3 to 5 percent of the dry weight of typical bacteria [34] (e.g., for *B. subtilis*, the percentage is 3 percent for vegetative cells and 5 percent for spores). Measured absolute fluorescence cross sections of *B. subtilis* spores are approximately proportional to the tryptophan content [35]. The peak emission of tryptophan is in the 320- to 360-nm range but depends upon its environment. Particles were generated with the IJAG with aerodynamic diameters of $\sim 5 \mu\text{m}$.

Figure 2 shows frequency-of-occurrence histograms of peak intensities of 1000 consecutive single-shot fluorescence spectra of individual tryptophan particles excited by a 266-nm laser. The insets in both (a) and (b) indicate the first 20 consecutive single-shot fluorescence spectra. In figure 2(a), the

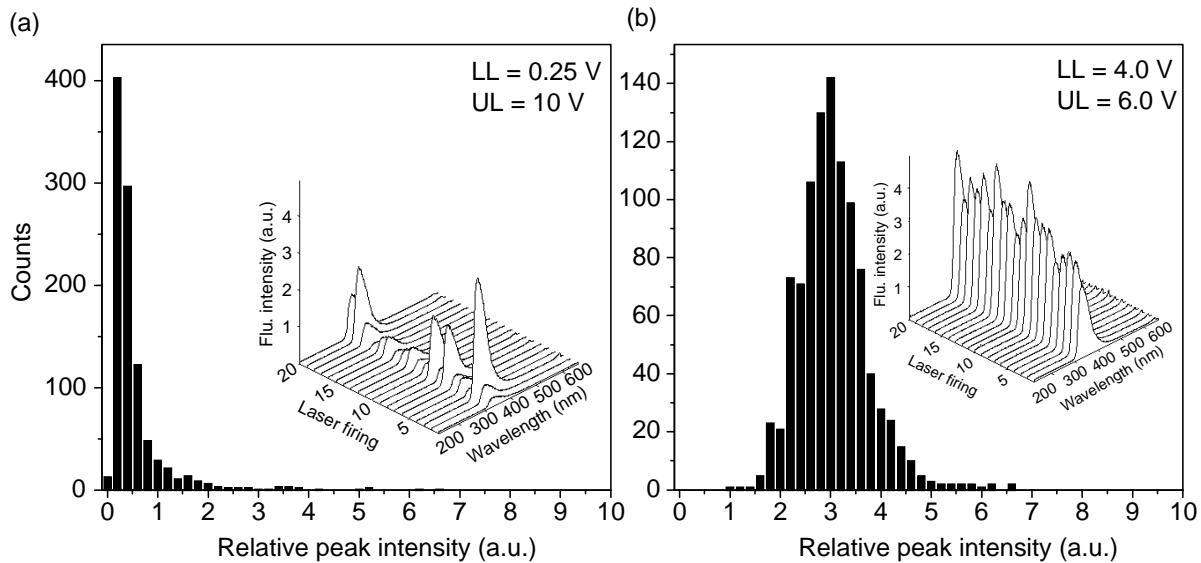


Figure 2. Frequency-of-occurrence histogram distributions of peak intensity for 1000 consecutive fluorescence spectra of individual tryptophan particles. Particles nominally $5 \mu\text{m}$ in diameter are excited with a pulsed 266-nm-wavelength laser (0.1 mJ/pulse, 70-ns duration, focused to $40 \mu\text{m}$ in diameter). In (a), discriminator levels for intensities of scattered light from diode-laser beams are wide (UL = 10 V, LL = 0.25 V), defining a sample volume that is larger than the UV probe laser beam. Consequently, a few strong fluorescence signals (corresponding to particles illuminated by the central portion of the UV beam), but mostly weak fluorescence signals (corresponding to particles in the wings of the UV beam), are measured. The resulting histogram is an inaccurate portrayal of the particle fluorescence. In (b), discriminator levels define a relatively narrow window (UL = 6 V, LL = 4 V), and all particles measured are illuminated by the central portion of the UV beam. Insets in both (a) and (b) indicate the corresponding spectra of the first 20 consecutive single-shot fluorescence spectra.

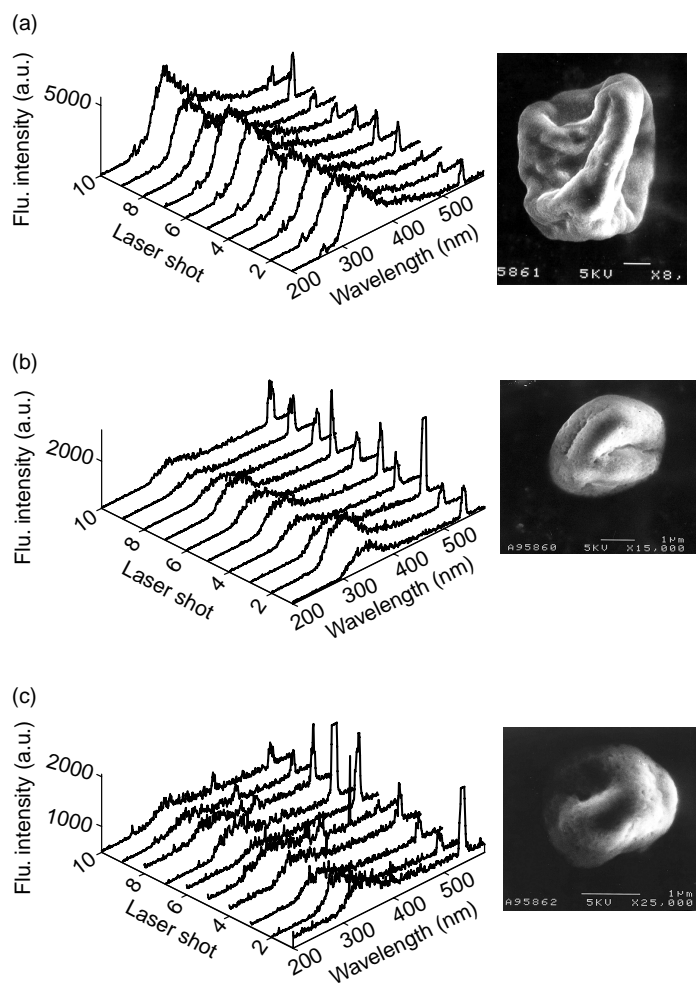
discriminator levels (for the PMT outputs proportional to the intensities of scattered light from the two diode-laser beams) are set to be wide: the preset upper (UL) and lower (LL) voltage levels of the two SCAs are set to be $UL = 10\text{ V}$ and $LL = 0.25\text{ V}$. The sample volume corresponding to this wide voltage window is large because particles that are several beam diameters from the center of the beams can give signals as large as 0.25 V . The resulting sample volume is larger than either the UV probe laser beam or the focal region of the reflective objective. Consequently, figure 2(a) shows a few spectra with strong fluorescence (corresponding to particles well illuminated in the central portion of the UV beam), but mostly spectra with weak fluorescence (corresponding to particles not well illuminated because not centered in the UV beam). The resulting histogram is an inaccurate portrayal of the particle fluorescence.

On the other hand, in figure 2(b), the discriminator levels are set to be relatively narrow ($UL = 6\text{ V}$, $LL = 4\text{ V}$). The resulting sample volume is smaller and lies more within the central portion of the UV beam and the focal region of the reflective objective. The distribution of peak intensities is approximately Gaussian, with the ratio of standard deviation to average intensity about 0.6. If the particle size distribution has a ratio of standard deviation to average radius of 0.15 (a typical value for the ink-jet generator), if the peak fluorescence is proportional to particle volume (not a bad assumption in this size range), and if the fluorescence is not saturated, then the ratio of the standard deviation of fluorescence to the average fluorescence should be about $3 \times 0.15 = 0.45$, if only the particle-size dispersion contributes to the deviation. That result would suggest that the instrument response contribution to the distribution is relatively small (ratio of standard deviation of intensity to intensity is about $0.6 - 0.45 = 0.15$). (The overall standard deviation is the sum of the standard deviations of the particle-size distribution and the instrument response width (caused by laser shot-to-shot intensity variations, etc).)

3.2 Spectra From Bacterial Particle Aggregates of Different Sizes

We tested the sensitivity and reliability of the system for bacteria using *B. subtilis*. Tryptophan makes up approximately 3 percent of the dry weight of *B. subtilis* and is usually the primary fluorophor in bacteria illuminated with 266-nm light. Therefore, we expect the overall fluorescence quantum efficiency of *B. subtilis* excited at 266 nm to be about 3 percent of that of pure tryptophan. Figure 3 shows 10 consecutive single-shot fluorescence spectra of *B. subtilis* vegetative cells (Sigma Chemical) in aggregates of nominal 5.0-, 2.3-, and 1.8-mm diam. For each cluster size, a typical SEM micrograph is shown on the right. The broad fluorescence peak (at 350 nm) is mainly from tryptophan, and the tail from 400 to 500 nm may be partially attributed to fluorescence from residues of the nutrient growth material and may have contributions from reduced nicotinamide compounds. The sharp peaks at 532 nm are from a leakage of the primary 532-nm beam that generates the 266-nm beam. The sharp peak in some of the 1.8- μm cluster spectra near

Figure 3. Single-particle laser-excited fluorescence spectra from clusters of airborne *B. subtilis* vegetative cells (Sigma) with nominal diameter (a) 5 μm , (b) 2.3 μm , and (c) 1.8 μm . Particles are illuminated with a single shot from a Q-switched 266-nm laser (frequency quadrupled Nd:YAG), with 0.1 mJ/pulse and 70-ns duration, focused to a 40- μm spot size. Electron micrographs of typical particles are shown for each size of cluster.



440 nm may be laser-induced plasma-excited atomic emission (possibly from nitrogen, calcium, or hydrogen), which only appears at high laser intensity. These data demonstrate that this system can capture the fluorescence spectra from single bacterial aerosols with sizes as small as 1.8 μm in diameter. Even for such small particles, the single-shot spectral lineshapes appear to be quite distinct and consistent.

3.3 Spectra of Similar Bacteria Prepared Under Different Conditions

Figure 4 shows single-particle, single-shot fluorescence spectra of clusters (aerodynamic diameter $\sim 5 \mu\text{m}$) of *B. subtilis* var. *niger* spores (Dugway) and *B. subtilis* var. *niger* cells (Sigma). A corresponding typical SEM micrograph for each sample is presented at the right of each spectrum. The spores exhibit more fluorescence in the 400- to 500-nm tail band, possibly because of impurities and differences in the ways the samples were prepared.

Figure 5 shows fluorescence spectra of *E. coli* strain DH5 (unstarved and four-month-starved samples). Aggregates of unstarved cells are about 4 μm in diameter, while aggregates of starved cells are about 2.5 μm in diameter. Starved sample data in figure 5 were obtained from the second pellet,

Figure 4. Single-particle, 266-nm laser (0.1 mJ/pulse, 70-ns duration, focused to 40- μm diam) excited fluorescence spectra from nominal 5- μm -diam clusters of *B. subtilis* var. *niger* spores (Dugway), and *B. subtilis* var. *niger* vegetative cells, (Sigma Chem). Electron micrographs of typical particles are shown for each sample.

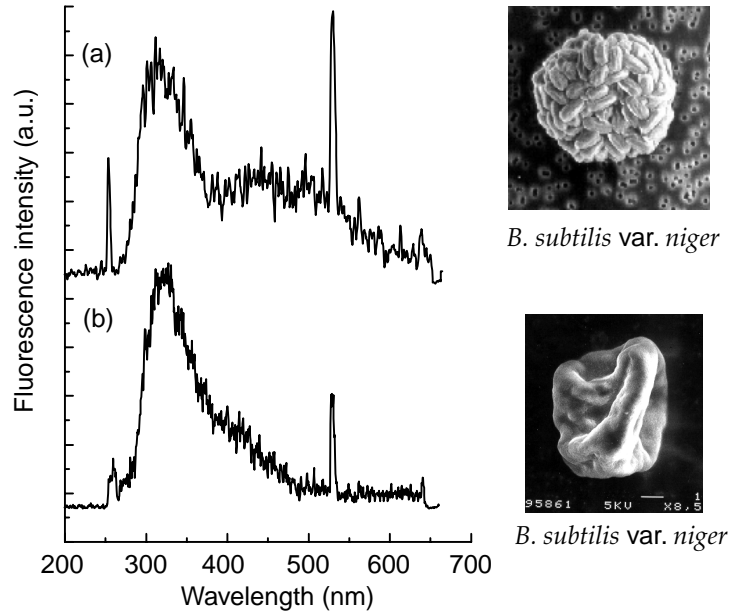
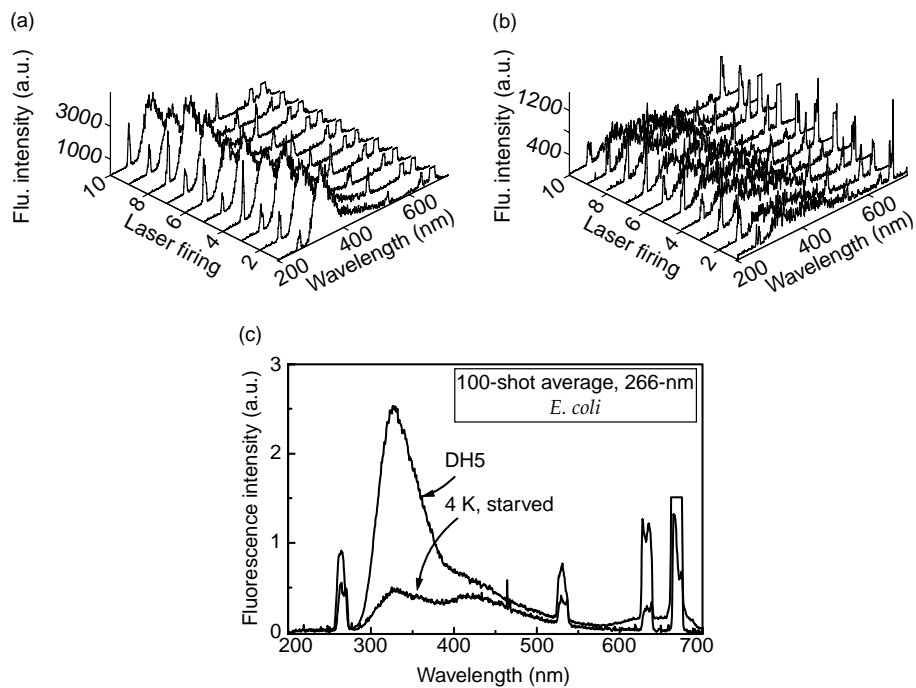


Figure 5. Fluorescence spectra of starved and unstarved *E. coli* strain DH5. Twenty consecutive single-shot, single-particle spectral results of (a) unstarved (4- μm diam) and (b) four-month-starved (2.5- μm diam) *E. coli* strain DH5, and (c) corresponding 100-shot (100 particles) averaged fluorescence spectra of *E. coli* strain DH5. Excitation is at 266 nm (0.085 mJ/pulse, 30-ns duration, focused to 40- μm diam).



centrifuged at 14 krpm for 15 min, that includes mostly smaller bacteria. Figures 5(a) and (b) show single-shot spectra while figure 5(c) shows the average spectrum from 100 consecutive shots. All *E. coli* single-shot fluorescence spectra show good spectral quality. These fluorescence results are qualitatively similar to those measured by a spectrofluorometer on a bulk liquid suspension of bacteria [30]. This similarity suggests that the method described here acquires accurate single-shot fluorescence spectra.

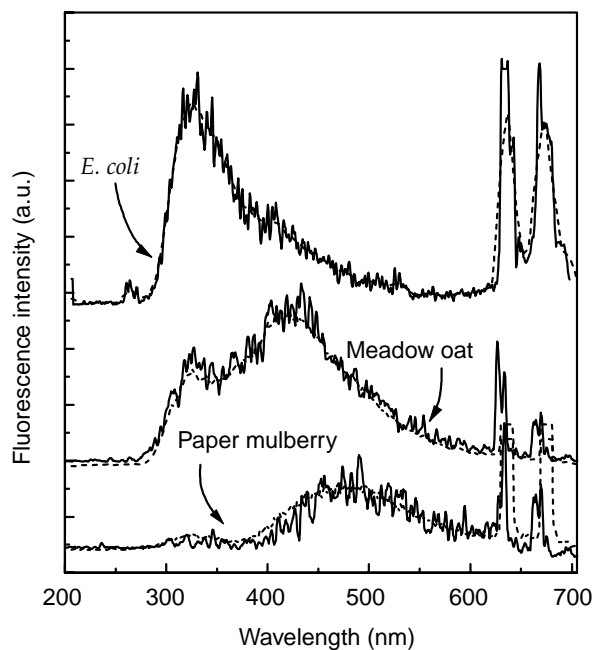
The spectral features of starved and unstarved cells are different: First, the absolute fluorescence peak intensity from the region of tryptophan emission (about 330 nm) is about five times larger in the unstarved samples. This ratio is comparable to the ratio of the volumes of the particles, i.e., $(4.0/2.5)^3 = 4.0$. Second, in the 400- to 500-nm range, the fluorescence of the starved bacteria is within 10 to 50 percent of the fluorescence of the unstarved bacteria. It appears that as the cells are starved, the tryptophan fluorescence per volume does not change markedly (it may decrease), but the fluorescence in the 400- to 500-nm range increases significantly, until the emission near 420 is nearly as large as the tryptophan peak. The compound(s) responsible for the increased emission in the 400- to 500-nm region have not yet been identified.

3.4 Spectra of Pollens and Bacteria

Figure 6 presents the single-shot, single-particle spectra of paper mulberry pollen, meadow oat pollen allergen, and *E. coli* (solid lines), excited by a 266-nm laser, as well as their corresponding 100-shot averaged results (dotted lines). The high quality of the single-shot spectral results shows that there are no substantive differences between the single-shot spectra and their corresponding 100-shot accumulation spectra. This confirms that the single-shot spectra of the individual bioaerosols represent the real spectral lineshape of the measured bioaerosols.

The spectra of paper mulberry pollen, meadow oat pollen allergen, and *E. coli* show clear differences. The highest intensity peaks in the pollen and pollen allergen spectra are located around 400 to 550 nm, but the *E. coli* emission is dominated by tryptophan (330 to 350 nm). The meadow oat

Figure 6. Single-shot, single-particle fluorescence spectra (solid lines) from nominal 5- μm -diam clusters of paper mulberry pollen, meadow oat pollen allergen, and *E. coli* (solid lines), and their corresponding 100-particle accumulation spectra (dotted lines). No difference in shape exists between single-shot spectra and their corresponding 100-shot accumulation spectra. Excitation is at 266 nm (0.085 mJ/pulse, 30-ns duration, focused to 40- μm diam).



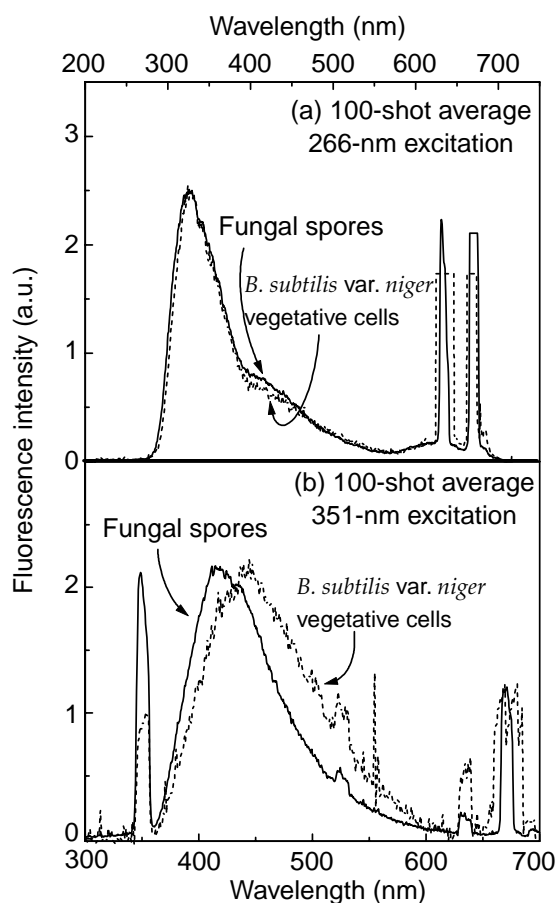
sample has significant emission in the tryptophan range, but the emission in this range from paper mulberry pollen emission is very low. These results, including those shown in figures 2 to 5 for bacteria, suggest that the relative intensities (tryptophan versus different bands in the longer wavelength emission) in single-shot fluorescence spectra could be useful for real-time discrimination between bacteria (in which the tryptophan peak is at least as large as any other peak in all of our measurements) and certain pollens and allergens (which have smaller tryptophan emission compared to that in the 400- to 500-nm band).

3.5 Spectra for Multiwavelength Excitation

Figure 7 shows fluorescence spectra of *B. subtilis* var. *niger* vegetative cells and fungal spores (*Aspergillus versicolor*), both 5 μm in diameter. The spectra in figure 7(a) are excited by 266-nm light and are similar for the two samples. Both spectra are dominated by the emission from the region of tryptophan emission.

In figure 7(b) the samples are excited with 351-nm light and the spectra are far less similar: The fluorescence peaks are at 450 nm for *B. subtilis* and 420 nm for the fungal spores. The photon energy of 351-nm light is too low to excite fluorescence from the aromatic amino acids (tryptophan and tyrosine are very poorly excited at wavelengths longer than about 305 nm), so these do

Figure 7. Fluorescence spectra of *B. subtilis* var. *niger* vegetative cells and *A. versicolor* fungal spores (both with nominal 5- μm diam). Excitation in (a) is with a 266-nm laser (0.085 mJ/pulse, 30-ns duration, focused to 40- μm diam), and in (b) is with a 351-nm laser (1.65 mJ/pulse, 120-ns duration, focused to 40- μm diam).



not contribute to the spectra in 7(b). The fluorescence is dominated by other compounds, which we conjecture may be flavins, nicotinamide nucleotides, secondary metabolites, and components of culture media (these may have more variability from sample to sample than do the amino acids). The fact that the spectra of the two samples are nearly the same at 266-nm excitation, but differ appreciably at 351-nm excitation, suggests that fluorescence spectra excited at different wavelengths may provide more discrimination among bioaerosols than would be possible with single-wavelength excitation.

3.6 Advantages and Limitations of This Technique

Our single-particle fluorescence-based method for detecting and partially classifying bioaerosols has several advantages. It should be capable of—

- (1) Detecting almost all bioaerosols at rates up to 50 to 1000 particles per second, if the particle diameters are on the order of 2 μm or larger (and possibly as small as 1 μm in diameter with less spectral resolution).
- (2) Determining the presence of bioaerosols of any origin without the use of reagents or prior knowledge of the types of aerosols that may be present.
- (3) When combined with pattern classification techniques, specifying bioaerosols into some as-yet-unspecified set of classes based on their sizes and spectra. These classes may discriminate between (for example) pollen allergens and bacteria, or bacteria generated under different conditions.
- (4) Detecting a very small concentration of biological particles mixed with a far higher concentration of nonbiological particles that either fluoresce very little or have a different spectral emission.

The approach also has some disadvantages:

- (1) Because our technique requires such a small sample volume (because we need to collect a large fraction of the emission and measure its spectrum), the rate at which we are able to sample the air is low. If the diameter of the sample region is about 20 μm and if the air traverses this region at 10 m/s (these are numbers comparable to what we use now), the sample rate is only 0.2 ml/min. Even if the particles are preconcentrated in air at a ratio of 1000:1 (e.g., if we use multiple virtual impactors), the equivalent sample rate is only 0.2 l/min, which is not high enough if the particles of interest have a concentration of 1/l or less. For such single-particle sampling, one would need greater preconcentration to keep the sampling time short (say, a few minutes). The flow rate can be increased in proportion to the sample-region cross section but at the cost of lower spectral resolution. We cannot significantly increase the excitation intensity, because nonlinear effects begin to appear [27].

(2) We do not expect UV-excited fluorescence spectra by themselves to be used to specifically identify airborne microorganisms, pollens, or allergens: there are too many possible types, possible mixtures, and possible growth conditions. This is a disadvantage, but it is the other side of the coin mentioned as advantage (2) above: The method should be capable of detecting all bioaerosols above 1 μm or so and do this without prior generation of specific molecules to detect specific proteins, nucleic acids, or polysaccharides.

4. Conclusion

We have obtained single-shot UV-excited intrinsic fluorescence spectra of individual flowing biological aerosol particles as small as 2 μm in diameter. The spectra measured from single bioaerosols have high signal-to-noise ratios and good spectral resolution and reveal small differences that may depend on the type of primary material in the bacteria and the method of preparation. With multiple-wavelength excitation (e.g., one wavelength within the absorption band for tryptophan and the other outside the band) and with pattern-recognition algorithms, this single-particle fluorescence-spectral technique may be useful for rapid detection and partial characterization of natural and anthropogenic indoor and outdoor aerosols.

Acknowledgments

New Mexico State University acknowledges financial support from the U.S. Army Research Laboratory (ARL, DAAL01-98-C0056). Yale University acknowledges the partial financial support from the U.S. Army Research Office (DAAG55-97-1-0349), the U.S. Air Force Research Laboratory and ARL (DAAL01-97-2-0128), and an Augmentation Award for Science and Engineering Research Training (AASERT) Fellowship (DAAG-97-1-0199) for S. Holler.

References

1. Lighthart, B., and L. D. Stetzenbach, Distribution of microbial bioaerosol. In *Atmos. Microb. Aerosols*, B. Lighthart and G. Mohr (ed.), New York: Chapman & Hall (1994), pp 68–98.
2. Matthias-Maser, S., and R. Jaenicke, Examination of atmospheric bioaerosol particles with radii greater than 0.2 micrometers. *J. Aerosol Sci.* **25** (1994), pp 1605–1613.
3. Madelin, T. M., Fungal aerosols—A review. *J. Aerosol Sci.* **25** (1994), pp 1405–1412.
4. Wathes, C. M., Bioaerosols in animal houses. In *Bioaerosols Handbook*, C. S. Cox and C. M. Wathes (ed.), Boca Raton: Lewis (1995), pp 547–577.
5. Burge, H., Bioaerosols in the residential environment. In *Bioaerosols Handbook*, C. S. Cox and C. M. Wathes (ed.), Boca Raton: Lewis (1995), pp 579–597.
6. Custovic, A., A. Fletcher, C.A.C., Pickering, H. C. Francis, R. Green, A. Smith, M. Chapman, and A. Woodcock, Domestic allergens in public places III: House dust mite, cat, dog, and cockroach allergens in British hospitals. *Clin. Exp. Allergy* **28** (1998), pp 53–59.
7. Fincher, E. L., Aerobiology and hospital sepsis. In *An Introduction to Experimental Aerobiology*, R. L. Dimmick and A. B. Akers (ed.), Wiley Interscience, New York (1969).
8. Zacharisen, M. C., A. R. Kadambi, D. P. Schlueter, V. P. Kurup, J. B. Shack, J. L. Fox, H. A. Anderson, and J. N. Fink, The spectrum of respiratory disease associate with metal working fluids. *J. Occup. Environ. Med.* **40** (1998), pp 640–647.
9. Heederik, D., R. Brouwer, K. Biersteker, and J.S.M. Boleij, Relationship of airborne endotoxin and bacteria levels in pig farms with the lung function and respiratory symptoms of farmers. *Int. Arch. Occup. Environ. Health* **62** (1991), pp 595–601.
10. Kullman, G. J., P. S. Thorne, P. F. Waldron, J. J. Marx, B. Ault, D. M. Lewis, P. D. Siegel, S. A. Olenchock, and J. A. Merchant, Organic dust exposures from work in dairy barns. *Am. Ind. Hyg. Assoc. J.* **59** (1998), pp 403–413.
11. Pillai, S. D., K. W. Widmer, S. E. Dowd, and S. C. Ricke, Occurrence of airborne bacteria and pathogen indicators during land application of sewage sludge. *Appl. Environ. Microbiol.* **62** (1996), pp 296–299.
12. Marchand, G., J. Lavoie, and L. Lazure, Evaluation of bioaerosols in a municipal solid waste recycling and composting plant. *J. Air Waste Manage. Assoc.* **146** (1996), pp 778–781.

13. Nel, A. E., D. Diaz-Sanchez, D. Ng, T. Hiura, and A. Saxon, Enhancement of allergic inflammation by the interaction between diesel exhaust particles and the immune system. *J. Allergy Clin. Immunol.* **102** (1998), pp 539–554.
14. Nevalainen, A., J. Pastuszka, F. Liebhaber, and K. Willeke, Performance of bioaerosol samplers: Collection characteristics and sampler design considerations. *Atmos. Environ.* **26A** (1992), pp 531–540.
15. Buttner, M. P., and L. D. Stetzenbach, Monitoring airborne fungal spores in an experimental indoor environment to evaluate sampling methods and the effects of human activity on air sampling. *Appl. Environ. Microbiol.* **59** (1993), pp 219–226.
16. Alvarez, A. J., M. P. Buttner, G. A. Toranzo, E. A. Dvorsky, A. Toro, T. B. Heikes, L. E. Mertikas-Pifer, and L. D. Stetzenbach, Use of solid-phase PCR for enhanced detection of airborne microorganisms. *Appl. Environ. Microbiol.* **60** (1994), pp 374–376.
17. Stewart, S. L., S. A. Grinshpun, K. Willeke, S. Terzieva, V. Ulevicius, and J. Donnelly, Effect of impact stress on microbial recovery on an agar surface. *Appl. Environ. Microbiol.* **61** (1995), pp 1232–1239.
18. Terzieva, S., J. Donnelly, V. Ulevicius, S. A. Grinshpun, K. Willeke, G. N. Stelma, and K. P. Brenner, Comparison of methods for detection and enumeration of airborne microorganisms collected by liquid impingement. *Appl. Environ. Microbiol.* **62** (1996), pp 2264–2272.
19. Reponen, T. A., S. V. Gizenko, S. A. Grinshpun, K. Willeke, and E. C. Cole, Characteristics of airborne actinomycete spores. *Appl. Environ. Microbiol.* **64** (1998), pp 3807–3812.
20. Franc, G. D. and P. J. DeMott, Cloud activation characteristics of airborne *Erwinia carotovora* cells. *J. Appl. Meteorol.* **37** (1998), pp 1293–1300.
21. Pinnick, R. G., S. C. Hill, P. Nachman, J. D. Pendleton, G. I. Fernandez, M. W. Mayo, and J. G. Bruno, Fluorescence particle counter for detecting airborne bacteria and other biological particles. *Aerosol Sci. Technol.* **23** (1995), pp 653–664.
22. Nachman, P., G. Chen, R. G. Pinnick, S. C. Hill, R. K. Chang, M. W. Mayo, and G. Fernandez, Conditional-sampling spectrograph detection system for fluorescence measurements of individual airborne biological particles. *Appl. Opt.* **35** (1996), pp 1069–1076.
23. Chen, G., P. Nachman, R. G. Pinnick, S. C. Hill, and R. K. Chang, Conditional-firing aerosol-fluorescence spectrum analyzer for individual airborne particles with pulsed 266-nm laser excitation. *Opt. Lett.* **21** (1996), pp 1307–1309.
24. Hairston, P. P., J. Ho, and F. R. Quant, Design of an instrument for real-time detection of bioaerosols using simultaneous measurement of particle aerodynamic size and intrinsic fluorescence. *J. Aerosol. Sci.* **28** (1997), pp 471–482.

25. Pinnick, R. G., S. C. Hill, P. Nachman, G. Videen, G. Chen, and R. K. Chang, Aerosol fluorescence spectrum analyzer for rapid measurement of single micrometer-sized airborne biological particles. *Aerosol Sci. Technol.* **28** (1998), pp 95–104.
26. Seaver, M., J. D. Eversole, J. J. Hardgrove, W. K. Cary, and D. C. Roselle, Size and fluorescence measurements for field detection of biological aerosols. *Aerosol Sci. Technol.* **30** (1999), pp 174–185.
27. Pan, Y. L., S. Holler, R. K. Chang, S. C. Hill, R. G. Pinnick, S. Niles, and J. R. Bottiger, Single-shot fluorescence spectra of individual micro-sized bio-aerosols illuminated by a 351-nm or 266-nm laser. *Opt. Lett.* **24**(2) (1999), pp 116–118.
28. Sambrook, J., E. F. Fritsch, and T. Maniatis, Appendix A: Bacterial media, antibiotics, and bacterial strains. In *Molecular Cloning: A Laboratory Manual*, C. Nolan (ed.), New York: Cold Spring Harbor 1989, pp A1–A13.
29. Seaver, M., D. C. Roselle, J. G. Pinto, and J. D. Eversole, Absolute emission spectra from *Bacillus subtilis* and *Escherichia coli* vegetative cells in solution. *Appl. Opt.* **37**(22) (1998), pp 5344–5347.
30. Roselle, D. C., M. Seaver, and J. D. Eversole, Changes in intrinsic fluorescence during the production of viable but nonculturable *Escherichia coli*. *J. Ind. Microbiol. Biotechnol.* **20** (1998), pp 265–267.
31. Kogure, K., U. Simidu, and N. Taga, A tentative direct microscopic method for counting living marine bacteria. *Can. J. Microbiol.* **25** (1979), pp 415–420.
32. Hobbie, J. E., R. J. Daley, and S. Jasper, Use of nucleopore filters for counting bacteria by fluorescence microscopy. *Appl. Environ. Microbiol.* **33** (1977), pp 1225–1228.
33. Bottiger, J. R., P. J. Deluca, E. W. Stuebing, and D. R. VanReenen, An ink-jet aerosol generator. *J. Aerosol Sci.* **29**, supplement 1 (1998), pp s965–966.
34. Murrell, W. G., Chemical composition of spores and spore structures. In *The Bacterial Spore*, A. Hurst and G. W. Gould (ed.), New York: Academic (1969) pp 218–231; Table III, p 221.
35. Faris, G. W., R. A. Copeland, K. Mortelmans, and B. V. Bronk, Spectrally resolved absolute fluorescence cross sections for bacillus spores. *Appl. Opt.* **36** (1997), pp 958–967.

Distribution

Admnstr
Defns Techl Info Ctr
ATTN DTIC-OCF
8725 John J Kingman Rd Ste 0944
FT Belvoir VA 22060-6218

Chairman Joint Chiefs of Staff
ATTN J5 R&D Div
Washington DC 20301

DARPA
ATTN S Welby
ATTN Techl Lib
3701 N Fairfax Dr
Arlington VA 22203-1714

Dir of Defns Rsrch & Engrg
ATTN DD TWP
ATTN Engrg
Washington DC 20301

Ofc of the Secy of Defns
ATTN ODDRE (R&AT)
The Pentagon
Washington DC 20301-3080

Ofc of the Secy of Defns
ATTN OUSD(A&T)/ODDR&E(R) R J Trew
3080 Defense Pentagon
Washington DC 20301-7100

Commanding Officer
ATTN NMCB23
6205 Stuart Rd Ste 101
FT Belvoir VA 22060-5275

AMCOM MRDEC
ATTN AMSMI-RD W C McCorkle
Redstone Arsenal AL 35898-5240

US Army TRADOC
Battle Lab Integration & Techl Dirctr
ATTN ATCD-B
FT Monroe VA 23651-5850

TECOM
ATTN AMSTE-CL
Aberdeen Proving Ground, MD 21005-5057

US Military Acdmy
Dept of Mathematical Sci
ATTN MAJ L G Eggen
West Point NY 10996-1786

Dir of Chem & Nuc Ops DA DCSOPS
ATTN Techl Lib
Washington DC 20301

US Military Acdmy
Mathematical Sci Ctr of Excellence
ATTN MADN-MATH MAJ M Huber
Thayer Hall
West Point NY 10996-1786

Dir for MANPRINT
Ofc of the Deputy Chief of Staff for Prsnl
ATTN J Hiller
The Pentagon Rm 2C733
Washington DC 20301-0300

SMC/CZA
2435 Vela Way Ste 1613
El Segundo CA 90245-5500

US Army ARDEC
ATTN AMSTA-AR-TD
Bldg 1
Picatinny Arsenal NJ 07806-5000

US Army Engrg Div
ATTN HNDED FD
PO Box 1500
Huntsville AL 35807

US Army ERDEC
ATTN SCBRD-RTE I Sindoni
ATTN SCBRD-RTE J Embury
ATTN SCBRD-RTE M Milham
Aberdeen Proving Ground MD 21005-5423

US Army Info Sys Engrg Cmnd
ATTN AMSEL-IE-TD F Jenia
FT Huachuca AZ 85613-5300

US Army Mis & Spc Intllgnc Ctr
ATTN AIAMS YDL
Redstone Arsenal AL 35898-5500

Distribution (cont'd)

US Army Natick RDEC Acting Techl Dir
ATTN SBCN-T P Brandler
Natick MA 01760-5002

US Army NGIC
ATTN Rsrch & Data Branch
220 7th Stret NE
Charlottesville VA 22901-5396

US Army Nuc & Cheml Agcy
7150 Heller Loop Ste 101
Springfield VA 22150-3198

US Army Simulation Train & Instrmntn
Cmnd
ATTN AMSTI-CG M Macedonia
ATTN J Stahl
12350 Research Parkway
Orlando FL 32826-3726

US Army Strtgc Defns Cmnd
ATTN CSSD H MPL Techl Lib
PO Box 1500
Huntsville AL 35807

US Army Tank-Automtv Cmnd RDEC
ATTN AMSTA-TR J Chapin
Warren MI 48397-5000

USAF Armstrong Lab Edgewood RDEC
ATTN AMSCB-AL B Bronk
ATTN SCBRD-RTE E Stuebing
ATTN SCBRD-RTE J R Bottiger
ATTN SCBRD-RTE S Christesen
Aberdeen Proving Ground MD 21010

Chief of Nav OPS Dept of the Navy
ATTN OP 03EG
Washington DC 20350

Nav Surf Warfare Ctr
ATTN Code B07 J Pennella
17320 Dahlgren Rd Bldg 1470 Rm 1101
Dahlgren VA 22448-5100

US Air Force Tech Appl Ctr
ATTN Hq AFTAC/TCC
ATTN S Gotoff
1030 South Highway A1A
Patrick AFB FL 32925-3002

Central Intllgnc Agcy
Dir DB Standard
ATTN OSS/KPG/DHRT
1E61 OHB
Washington DC 20505

US Dept of Energy
ATTN Techl Lib
Washington DC 20585

Univ College Galway
Depart of Experimental Physics
ATTN S G Jennings
Ireland

New Mexico State Univ
Depart of Physics
ATTN R Armstrong
Room 256 Gardiner Hall
Las Cruces NM 88003

Hicks & Assoc Inc
ATTN G Singley III
1710 Goodrich Dr Ste 1300
McLean VA 22102

US Army Rsrch Lab
ATTN SCBRD-RTE R Smardzewski
Aberdeen Proving Ground MD 21010

Director
US Army Rsrch Lab
ATTN AMSRL-RO-D JCI Chang
ATTN AMSRL-RO-EN W Bach
ATTN AMSRL-RO-EN B Mann
PO Box 12211
Research Triangle Park NC 27709-2211

Distribution (cont'd)

US Army Rsrch Lab

ATTN AMSRL-CI-AI-R Mail & Records

Mgmt

ATTN AMSRL-CI-AP Techl Pub (2 copies)

ATTN AMSRL-CI-LL Techl Lib (2 copies)

ATTN AMSRL-CI-CI D Hillis

ATTN AMSRL-CI-EM J D Pendleton

ATTN AMSRL-CI-EM S Hill (10 copies)

ATTN AMSRL-CI-EM R Pinnick (20 copies)

Adelphi MD 20783-1197

REPORT DOCUMENTATION PAGE			<i>Form Approved</i> OMB No. 0704-0188	
Public reporting burden for this collection of information is estimated to average 1 hour per response, including the time for reviewing instructions, searching existing data sources, gathering and maintaining the data needed, and completing and reviewing the collection of information. Send comments regarding this burden estimate or any other aspect of this collection of information, including suggestions for reducing this burden, to Washington Headquarters Services, Directorate for Information Operations and Reports, 1215 Jefferson Davis Highway, Suite 1204, Arlington, VA 22202-4302, and to the Office of Management and Budget, Paperwork Reduction Project (0704-0188), Washington, DC 20503.				
1. AGENCY USE ONLY (Leave blank)		2. REPORT DATE February 2001		3. REPORT TYPE AND DATES COVERED Progress 7/1/1998 to 3/1/1999
4. TITLE AND SUBTITLE Fluorescence Spectra of Individual Flowing Airborne Biological Particles Measured in Real Time			5. FUNDING NUMBERS DA PR: B53A PE: 61102A	
6. AUTHOR(S) R. G. Pinnick, S. C. Hill, S. Niles (ARL), Y.-L. Pan (New Mexico State Univ.), S. Holler, R. K. Chang (Yale Univ.), J. R. Bottiger (U.S. Army Edgewood Chemical Biological Center), B. V. Bronk (U.S. Air Force Research Laboratory), D. C. Rozelle, J. D. Eversole, and Mark Seaver (Naval Research Laboratory)				
7. PERFORMING ORGANIZATION NAME(S) AND ADDRESS(ES) U.S. Army Research Laboratory Attn: AMSRL-CI-EE email: shill@arl.army.mil 2800 Powder Mill Road Adelphi, MD 20783-1197			8. PERFORMING ORGANIZATION REPORT NUMBER ARL-TR-1961	
9. SPONSORING/MONITORING AGENCY NAME(S) AND ADDRESS(ES) U.S. Army Research Laboratory 2800 Powder Mill Road Adelphi, MD 20783-1197			10. SPONSORING/MONITORING AGENCY REPORT NUMBER	
11. SUPPLEMENTARY NOTES ARL PR: 9FEJ71 AMS code: 61110253A11				
12a. DISTRIBUTION/AVAILABILITY STATEMENT Approved for public release; distribution unlimited.			12b. DISTRIBUTION CODE	
13. ABSTRACT (Maximum 200 words) The UV-excited fluorescence spectra of individual flowing biological aerosol particles as small as 2 μm in diameter have been measured in real time (rates up to 10 particles per second). The particles are illuminated with a single shot from a Q-switched 266- or 351-nm laser. The signal-to-noise ratio and resolution of the spectra are sufficient for observing small line-shape differences among various types of bioaerosols (e.g., bacteria versus pollens) and between the same types of bioaerosol prepared under different conditions (e.g., the unstarved and four-month-starved <i>E. coli</i> strain DH5). Multiple-wavelength excitation provides additional information for distinguishing bioaerosols based on their fluorescence spectra.				
14. SUBJECT TERMS bioaerosols, aerosol detection, aerosol fluorescence, biological aerosols, fluorescence spectroscopy, single-particle spectroscopy			15. NUMBER OF PAGES 29	
			16. PRICE CODE	
17. SECURITY CLASSIFICATION OF REPORT Unclassified	18. SECURITY CLASSIFICATION OF THIS PAGE Unclassified	19. SECURITY CLASSIFICATION OF ABSTRACT Unclassified	20. LIMITATION OF ABSTRACT UL	